3 Biotech (2017) 7:174
DOI 10.1007/s13205-017-0830-6

ORIGINAL ARTICLE

Fabrication and characterization of chitosan nanoparticles and collagen-loaded polyurethane nanocomposite membrane coated with heparin for atrial septal defect (ASD) closure

Eva Kaiser[1,2] · Saravana Kumar Jaganathan[3,4,5] · Eko Supriyanto[1] · Manikandan Ayyar[6]

Received: 15 February 2017 / Accepted: 1 June 2017 / Published online: 29 June 2017

Abstract Atrial septal defect (ASD) constitutes 30–40% of all congenital heart diseases in adults. The most common complications in the treatment of ASD are embolization of the device and thrombosis formation. In this research, an occluding patch was developed for ASD treatment using a well-known textile technology called electrospinning. For the first time, a cardiovascular occluding patch was fabricated using medical grade polyurethane (PU) loaded with bioactive agents namely chitosan nanoparticles (Cn) and collagen (Co) which is then coated with heparin (Hp). Fourier transform infrared spectrum showed characteristic vibrations of several active constituents and changes in the absorbance due to the inclusion of active ingredients in the patch. The contact angle analysis demonstrated no significant decrease in contact angle compared to the control and the composite patches. The structure of the electrospun nanocomposite (PUCnCoHp) was examined through scanning electron microscopy. A decrease in nanofiber diameter between control PU and PUCnCoHp nanocomposite was observed. Water uptake was found to be decreased for the PUCnCoHp nanocomposite against the control. The hemocompatibility properties of the PUCnCoHp ASD occluding patch was inferred through in vitro hemocompatibility tests like activated partial thromboplastin time (APTT), prothrombin time (PT) and hemolysis assay. It was found that the PT and APTT time was significantly prolonged for the fabricated PUCnCoHp ASD occluding patch compared to the control. Likewise, the hemolysis percentage was also decreased for the PUCnCoHp ASD patch against the control. In conclusion, the developed PUCnCoHp patch demonstrates potential properties to be used for ASD occlusion.

Keywords Atrial septal defect · Blood compatibility · Textile technology · Electrospinning · Cardiac patch · Nanofibers

✉ Saravana Kumar Jaganathan
saravana@tdt.edu.vn

[1] Faculty of Biosciences and Medical Engineering, Universiti Teknologi Malaysia, 81310 Johor Bahru, Malaysia

[2] Ilmenau Institute of Biomedical Engineering and Computer Science, Technical University of Ilmenau, 98693 Ilmenau, Germany

[3] Department for Management of Science and Technology Development, Ton Duc Thang University, Ho Chi Minh City, Vietnam

[4] Faculty of Applied Sciences, Ton Duc Thang University, Ho Chi Minh City, Vietnam

[5] IJN-UTM Cardiovascular Engineering Centre, Faculty of Biosciences and Medical Engineering, Universiti Teknologi Malaysia, 81300 Skudai, Johor, Malaysia

[6] Department of Chemistry, Bharat Institute of Higher Education and Research, Bharat University, Chennai, Tamilnadu 600073, India

Introduction

Postoperative erosion of the aortic or atrial wall is a dreadful complication of percutaneous septal defect closure using an atrial septal occluder (ASO). Erosion event is the chief concern since it occurs in a vulnerable pediatric population. It decreases the ability to predict those patients who may be at high risk and may lead to an urgent life threatening event (Fornell 2013). These events occur in almost 1–3 of every 1000 patients implanted with the ASO. According to latest survey, a massive 234,103 ASO devices were sold worldwide. The risks allied with device removal

surgery may be equal to or higher than the risk of erosion (Fornell 2013). A review was performed for determining the occurrence of erosion events in the ASO. It was found that there are 25 pertinent articles ascertaining the cases of cardiac erosion coupled with the ASO and 21 independent surgically confirmed cases (case reports), 1 suspected event and 79 distinct events reported in case series and review articles (Crawford et al. 2012). Stroke due to late ASO thrombosis was reported in a recent study. Further, the occurrence of recurrent neurologic events in these same studies has ranged between 0 and 2.6% (Korabathina et al. 2012). Moreover, allergy to nickel occurs in up to 15% of the population where adverse events observed in 37 patients with ASO (Wertman et al. 2006).

Fully absorbable ASO occlude may resolve the concerns relating to permanent devices by eliminating utilization of non-degradable materials specifically the metal. A biodegradable occluder not only closes the hole, but also confers a temporary scaffold for the in-growth of host tissue to cover the device and the defect underneath. Ultimately, the device may degrade into nontoxic ingredients and then be fully absorbed thereby leaving the "native" tissue behind. This notion can minimize the potential for future complications triggered by the presence of a foreign body (Liu et al. 2011). Polyurethane (PU) is a commonly available polymer and it mainly contains urethane linkage. The urethane linkage is formed by the reaction between isocyanates and aldols. The PU has higher elasticity, toughness, resistance to oxidation, tear and humidity. Further, the cost involved in production of polyether derivatives is low which can reduce the cost associated with metallic frames made from nitinol which is a shape memory alloy (SMA). The PU is a shape memory polymer capable of 100% shape regain even when it is stretched above its glass transition temperature. Farzaneh et al. deformed the polyurethane in the glass transition zone or at a higher temperature and found that the polymer completely regains its shape after mechanical deformation making polyurethane an excellent substitute for the nitinol (Farzaneh et al. 2013). The presence of hard domains plays a vital role in shaping the inelastic properties of PU by increasing the crosslinking of the polymer chains. With the improved volume fraction of domains dominated by hard segments, these domains are better cross-linked and interconnected thereby making them a promising polymer for occluder. The commercial elastomeric polyurethane (Tecoflex EG-80A) which is used in this research was a medical grade PU and already used in the clinical application of vascular grafts because of its elastomeric property and good compatibility. In addition, its slow degradation rate is inferred to match with the synthesis of ECM components and cardiac tissue regeneration process for the closure of ASD (Detta et al. 2010).

There are several studies indicating that the chitosan nanoparticles (Cn) improve the mechanical strength of the matrix in which they embedded. For instance, the Cn were found to improve the mechanical property of hydroxypropyl methylcellulose (HPMC) films suggesting that Cn are promising fillers to bolster the strength of the matrix material (Moura et al. 2008, 2009). Likewise, in another study Cn were found to bolster the mechanical properties of different pectin-based films significantly (Lorevice et al. 2015). The electrospun fiber mats have been reported to be a promising solution for various biomedical applications (Balaji et al. 2015; Sill and Recum 2008). Similarly, in another work collagen (Co) was electrospun to a degradable occluder membrane by Liu et al. (2011). Co provides a natural extracellular matrix for many body tissues like skin, bone or ligament of connective tissue. As an endogenous product, it is relatively non-immunogenic and does not evoke adverse reactions (Liu et al. 2011). The procedure of coating a biomaterial to improve its blood compatibility is a facile approach which has shown impressive results (Gorbet and Sefton 2004). Due to its anticoagulant properties, heparin (Hp) has been widely applied to the surfaces of vascular implants. The Hp possesses good anti-thrombogenic properties making it a putative candidate as a coating material of cardiovascular biomaterials (Chen et al. 2010; Klement et al. 2002). Hence, a novel patch comprising PUCnCoHp might lead to better engineered properties compared to the conventional PU patch.

In this study, PU nanofibrous membrane loaded with Cn and Co was fabricated using electrospinning technique. Later, this membrane was coated with Hp with an intention to improve its blood compatibility. The final PUCnCoHp nanocomposite membrane was characterized and its blood compatibility properties were assessed.

Experimental

Materials

The necessary chemicals required for conducting the research were obtained from the companies listed as following. The kits for activated partial thromboplastin time (APTT) and prothrombin time (PT) were from Diagnostic Enterprises (Parwanoo, India). They were used without any further purification. Commercial medical grade aliphatic, polyether-based TPU (Tecoflex EG 80A injection grade, Lubrizol Advanced Materials, Inc., Thermedics Polymer Products, USA) in bead form was donated by Indian Institute of Technology, Kharagpur, India. The chitosan powder was bought from BioBasic Inc. with a purity of more than 90% cps. Collagen type 1 and 3 was obtained from NeoCell Corporation. Heparin 5000 was purchased

from Ratiopharm GmbH, Germany. Analytical grade dimethylformamide (DMF) and glacial acetic acid (100%) were bought from Merck AG, Germany. The sodium tripolyphosphate (TPP) in technical grade was obtained from Sigma Aldrich, Germany.

Chitosan nanoparticles synthesis

The series of tests performed in this study are represented in Fig. 1. The Cn were prepared following the method reported by Qi et al. (2004). Glacial acetic acid was diluted with deionized water to obtain 1% v/v acetic acid. Chitosan was dissolved using this to obtain 0.5% (w/v) solution. The pH (HI 8424, Hanna Instruments) of the solution was found to be 3.36 which was then raised to 4.64 with the addition of 2.5% NaOH (1.9 ml). The triphenyl phosphate (TPP) solution, mixed to 0.25% (w/v) with deionized water, was added dropwise to the chitosan solution in a ratio of 1:3 under magnetic stirring to obtain chitosan nanoparticles.

Electrospinning solution preparation

Electrospinning solution was prepared using the Cn (1%) and Co (2%) in combination with PU (4%) in the ratio of 9:0.5:0.5 (PU:Cn:Co). The pure PU patch and the composite patches were spun at a flow rate of 1 ml/h with the applied voltage of 19 kV. After completing the spinning process, patches were dried at room temperature for 2 days.

Characterization

Spectral analysis

The Cn were analyzed using the UV–Vis spectrophotometer (GENESYSTM10S, Thermo Electron Scientific Instruments, USA). The spectrum was recorded in the range of 180–800 nm using absorbance mode. The measured absorbance gives information about bonding conditions within the molecule. The scan speed was set to medium and the measurement interval was 1.0 nm. Finally, a plot between the wavelength and the absorbance was obtained through the integrated software within the equipment.

Fourier transform infrared spectroscopy

The Fourier transform infrared spectroscopy (FTIR) spectroscopy was performed using the Nicolet iS5 (Thermo Electron Scientific Instruments, USA) system. FTIR spectra of PU, composite patches, Cn and Co were obtained. The spectrum was recorded over the range of 600–4000 cm^{-1} at 32 scans per minute with a resolution of 4 cm^{-1} in absorbance mode. The ATR crystal used was zinc/selenium which was coupled with the NICOLET IS5 spectrometer. After recording, the spectra were baseline corrected and normalized using OMNIC Specta software (Thermo Scientific, USA) to identify the characteristic peaks and differences.

Contact angle assay

Changes concerning the wettability of the PU composite patch were studied using the VCA Optima (AST Products, Inc., USA) contact angle measurement unit. The samples were cut into rectangular shape (1 cm × 5 cm) and placed on the stage. The syringe, filled with distilled water, was arranged close to the sample and a water droplet (size 1 µl) was placed on the PU control or the composite samples. The contact angle was measured manually with the aid of the optical system and the corresponding VCA software. The camera parameters were set to 70% concerning the brightness, the contrast was set at 60% and the resolution was at 640 × 480, to assure an evaluable image. The experiment was conducted at room temperature.

Scanning electron microscope

Scanning electron microscope (SEM) analysis was performed to evaluate the surface of the patch and to evaluate the diameter of the nanofibers. Therefore, a small piece of the respective membrane was cut and pasted on a coin by using double-sided tape. The sample was then adjusted on the stage and sputter coated with gold to obtain an electrically conductive surface using the BioRad Polaron Division. To obtain the surface images, the Hitachi Table Top Microscope (TM3000) coupled with EDS analysis system was used. The samples were imaged at a magnification of 6000× and 7000×. The average diameter and standard deviation (SD) of the PU and the composite fibers were determined using GIMP image analysis system ($n = 10$).

Blood compatibility assessment

All the experimental procedures incorporated in the treatment of blood were approved by the Faculty of Biosciences and Medical Engineering, Universiti Teknologi Malaysia with ref no: UTM.J.45.01/25.10/3Jld.2(3). Eight ml blood was taken from a voluntary donor and stored in coagulation blood collective tubes. The tubes were stored at 4.5 °C in the refrigerator before any further use. For the coagulation assays, 4 ml whole blood was centrifuged at 3000 rpm for 10 min. The supernatant platelet-poor plasma (PPP) was used for further experimentation. The patches were placed in a 96-well plate for conducting the APTT and PT.

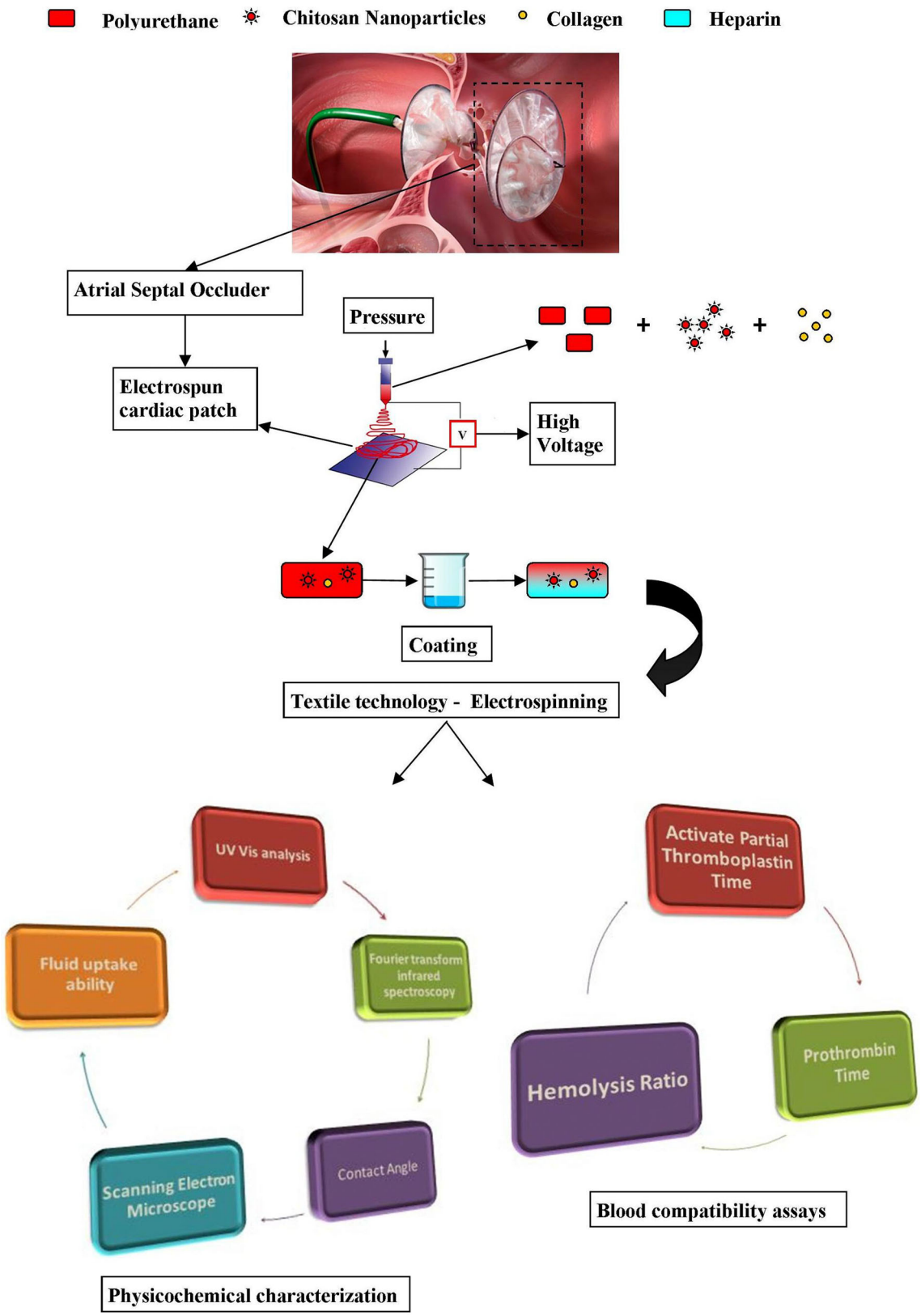

Fig. 1 Schematic representation of this study

Activated partial thromboplastin time

Activated partial thromboplastin time is a highly reliable basic blood compatibility test, suitable for detecting the capability of blood coagulation through the intrinsic coagulation pathway. It helps us to understand how the contact of the blood with biomaterials affects the activation of the coagulation pathway. The samples were thoroughly washed with deionized water, incubated in PBS for 30 min at 37 °C. The substrates were pre-incubated with 50 µL PPP at 37 °C and then activated by incubating with 50 µL rabbit brain cephalin (ratio 1:1) for 2 min. For initiating clot formation, 50 µL calcium chloride was added to the mixture. The time for initiation of clot formation was measured immediately using a stopwatch (Jaganathan et al. 2017; Manikandan et al. 2017). A steel needle of diameter 23 mm was used to investigate the formation of clot.

Prothrombin time

Similarly, the time taken for the formation of the clot through extrinsic pathway was estimated through prothrombin assay. The PT is expressed as a ratio called international normalized ratio (INR) in which the time for the sample clot is relative to the control sample. The INR normally ranges between 0.8 and 1.4 (Eyre and Gamlin 2010). In this assay, the samples were rinsed in deionized water and incubated in PBS at 37 °C for 30 min. Rabbit brain NaCl–thromboplastin (0.9%) containing Ca^{2+} was added to the substrate, pre-incubated in PPP (50 µL). Then, the mixture was slowly stirred using a steel needle (ø23 mm) and the time taken for the onset of fibrin formation was determined using a stopwatch (Jaganathan et al. 2017; Manikandan et al. 2017).

Hemolysis ratio

The hemolysis ratio analyzes the impact on red blood cells (RBC) when they interact, e.g., biomaterials evokes any lysis of the RBC. The samples were cut into squares (10 mm × 10 mm) before placing into 0.8 ml citrated whole blood diluted in 1 ml of saline. Subsequently, a positive and a negative control were prepared. The positive control consisted of 0.8 ml of blood with 1 ml distilled water; whereas the negative control was physiological saline. The incubation time was 60 min at a temperature of 37 °C. The mixtures were centrifuged at 3000 rpm for 10 min and the hemolytic percentage was determined using photometric analysis of the supernatant. Therefore, 0.8 ml of the supernatant was placed into a 1-ml cuvette for measuring the absorbance. The absorbance of the supernatant was measured at 542 nm to quantify the amount of hemoglobin released in order to estimate the eventual degree of damage to the RBC (Amarnath et al. 2006; Wright 2006). The hemolysis ratio was calculated using the below mentioned formula. TS is the absorbance of the test sample, whereas NC and PC are the absorbance's of the negative and positive control, respectively:

$$\mathrm{H} = \frac{\mathrm{TS} - \mathrm{NC}}{\mathrm{PC} - \mathrm{NC}}. \quad (1)$$

Fluid uptake ability

Water uptake ability of the PU and composite patches over a certain time span was measured as follows. Samples were cut into 10 mm × 10 mm and placed in phosphate buffered saline at a pH adjusted to 7.4. The temperature was kept stable at room temperature. The patches were immersed in water for the time span of 6, 12 and 24 h. After immersion, the patches were then placed on to a fresh absorbing paper for 30 s and their weight was measured. The fluid uptake ability (FUA, %) of the composite patch and the control sample was calculated as a percentage of water loss per unit weight:

$$\mathrm{FUA}\,(\%) = \frac{W_\mathrm{w} - W_0}{W_\mathrm{w}} \times 100,$$

where W_w is the wet weight of the nanofiber and W_0 is the dry weight of the nanofiber (Zhou and Gong 2008).

Statistical analysis

All quantitative experiments were performed three times ($n = 3$) for each sample. The statistical analysis was carried out using one-way ANOVA method and all results are expressed as mean ± standard deviation.

Results and discussion

Characterization

Synthesis of chitosan nanoparticle: UV–Vis analysis

The peak or the highest absorption (absorbance = 1) was found at a wavelength of 289 nm which is depicted in Fig. 2. This peak confirms the formation of nanoparticles as reported recently by Liu and Gao (2009). The authors found a similar peak in this wavelength in UV–Vis and ascribed it to the color change from transparent to opal during the addition of the TPP to the chitosan solution. Likewise, researchers reported that distilled water is commonly used as a chemical-blowing agent. It evokes an exothermic reaction resulting in the formation of highly viscous product when it gets in contact with PU (Thirumal

et al. 2008). Hence, a minimal water level in the Cn will make the final composite solution spinnable.

Fourier transform infrared spectroscopy

The recorded FTIR result of Co and Cn is given in Fig. 3. Likewise, the recorded FTIR spectrum, which compares the PU control sample with the PU composite patch with and without Hp coating is displayed in Figs. 4 and 5, respectively. The FTIR spectrum of electrospun PU nanofibers displayed similar characteristic absorption bands compared to the composite patches with some differences. A variation in the intensities were noted for both control and coated samples at wave numbers 754, 794, 838, 1025, 1088, 1270, 1285, 1335, 1425, 1440, 1459, 1492, 1719 and 2893 cm^{-1}. The FTIR spectroscopy of PU has characteristic absorption bands at ≈3290, ≈1700, ≈1600, ≈1525, ≈1220 cm^{-1}, which are associated with different groups in the PU molecule *v* (–N–H), *v*(–C=0), *v*(–C–N), *v*(–C=C), *v*(–C–O–C), respectively (Yang et al. 2011). These peaks are all represented in the PU control spectrum. The composite shows some additional peaks and changes with regard to the absorbance. Between 600 and 800 cm^{-1} the absorbance of the patch is less than the one of the control patch and similar observations were reflected at around 1100, 1200 and 1650 cm^{-1}. In contrast, at the wavelength

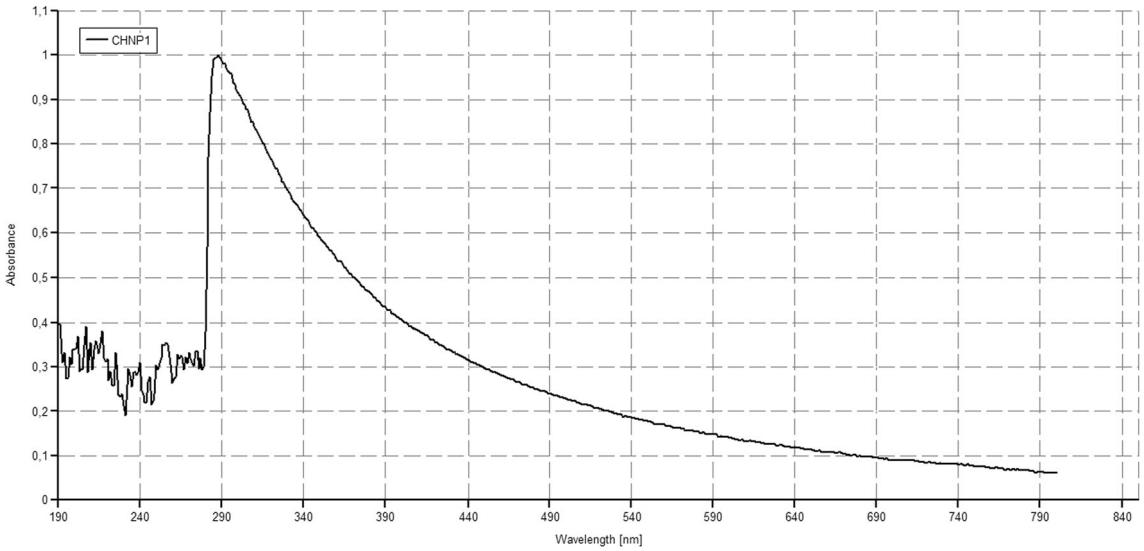

Fig. 2 Spectral analysis of the Cn using UV–Vis with a maximum absorption at 289 nm

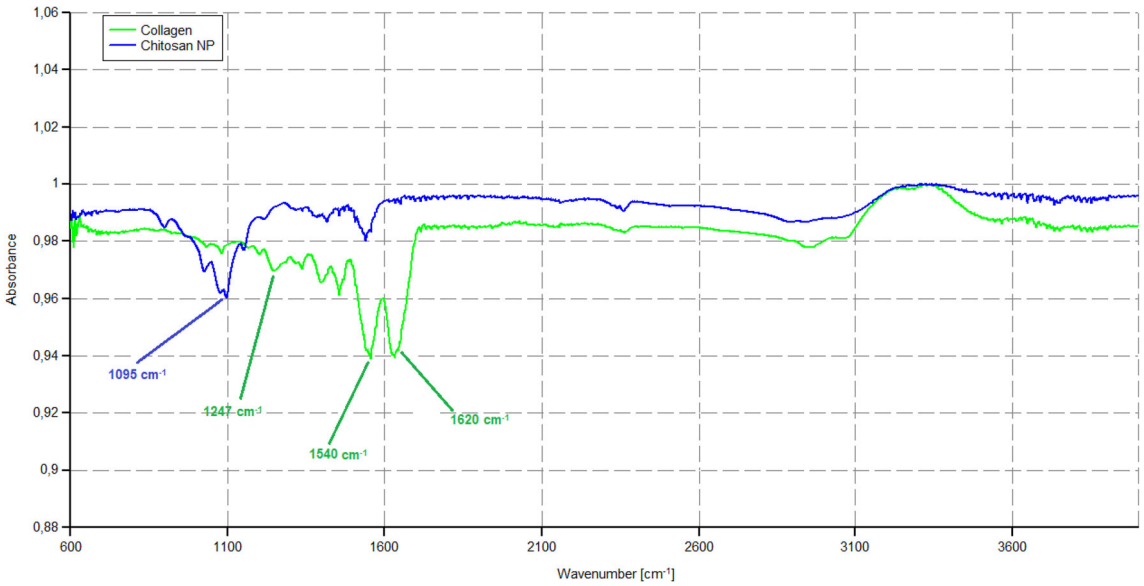

Fig. 3 Fourier transform infrared spectroscopy of the patch ingredients Co and Cn

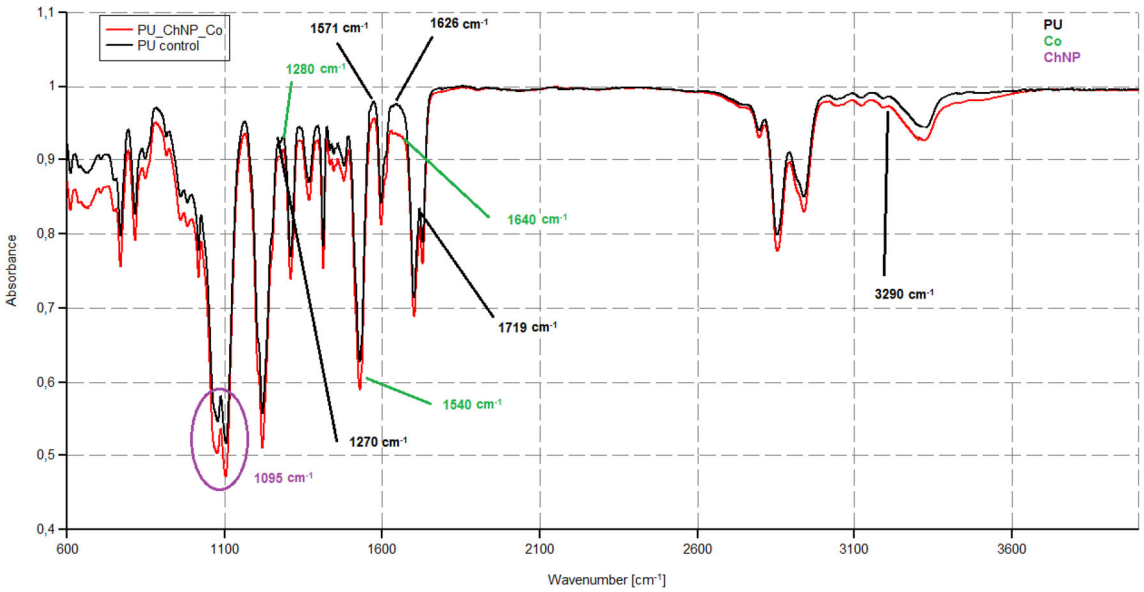

Fig. 4 FTIR of the PU patch in comparison with the PU composite patch. The changes in the functional groups are highlighted

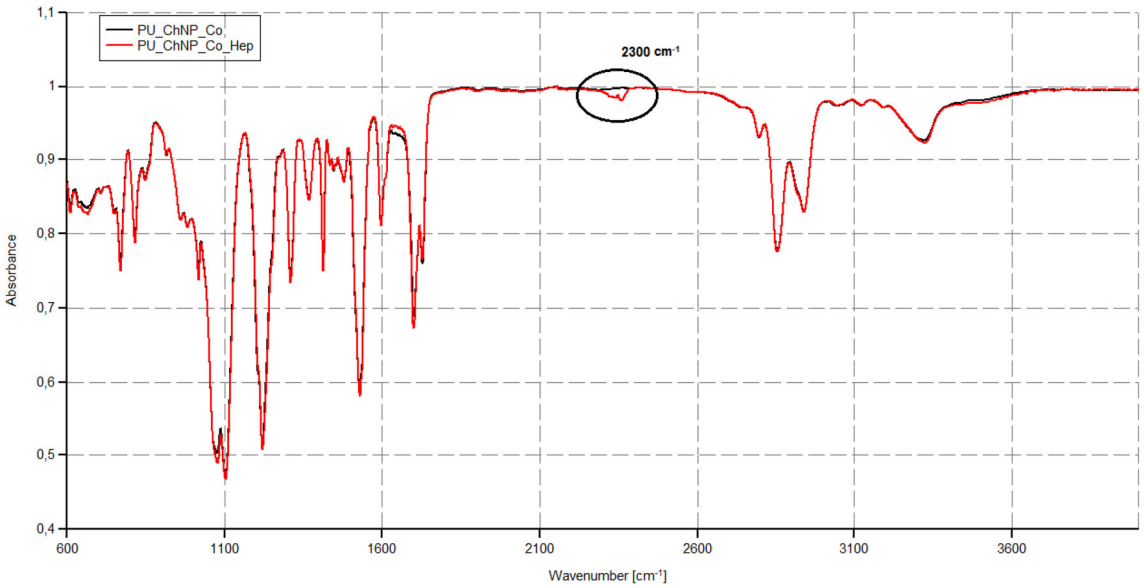

Fig. 5 Fourier transform infrared spectroscopy of the PU composite in comparison with the composite coated with Hp

of $\approx$3320 cm^{-1} the composite patch shows a higher absorption. The Co was used as reference sample and showed peaks at 1640, 1540 and 1280 cm^{-1}, which represent the amide I, II and III bands of Co (Wong and Badri 2012). The Hp-coated patch shows the same differences as the uncoated composite compared to the reference sample, except a peak at 2300 cm^{-1}.

Besides that, when the composite PUCnCo was compared with the PU, it did not show any major alteration in the functional groups due to the small amount of active ingredients in the patch. The composite patch shows a characteristic absorption band for Cn at the wavenumber 1095 cm^{-1} ν(C–=). The changes at the wave number 1650 is due to the functional group of (C=0) of the Cn and the lower absorption at 1100 cm^{-1} is caused by the ν(C–O–C), respectively (Rinaudo 2006). The composite shows some shifts concerning the absorbance, which is attributed to the Cn for the wavenumbers around 600–700 cm^{-1}. Due to the addition of Co, the absorption shifts at 1600 cm^{-1}, the peaks at 1540, 1456 and 1363 cm^{-1} also indicate the presence of Co and represent its triple helix structure (Pedicini and Farris 2003). The peak in the Hp-coated sample at 2300 cm^{-1} peak refers to the S–H stretch in the Hp which was absent in the other samples. Likewise, the

changes at 1256 cm^{-1} as well as the lower absorption at 1078 cm^{-1} are characteristic for the $–OSO_3(S=O)$ indicating the presence of Hp (Chen et al. 2016). Lastly, the peak at 3320 cm^{-1} indicates a change concerning the hydrophilic properties of the patch due to Co and Cn where both show a peak in their spectrum at the mentioned wavenumbers.

Contact angle

The contact angle was expressed as mean value of the three measurements and the standard deviation as displayed in Fig. 6. The mean contact angle calculated for the PU reference was 84:23° ± 1.06, the composite without coating had a mean contact angle of 87:62° ± 3.73 and the heparin-coated patch showed a contact angle of 90:42° ± 1.41. The statistical analysis did not show a significant ($p < 0.05$) difference between the control and the composite patch. Surfaces with suitable hydrophilic properties show a better cell adherence and support an effective spread compared to hydrophobic surfaces. The wettability, or contact angle assay, is used to evaluate the hydrophilicity of the sample surface (Wang et al. 2015). To prove the wettability of the developed patch, the contact angle is used as a common tool in several studies. PU has not always shown the best biocompatibility in application, but there are several methods to improve the wettability, e.g., adding, coating or blending the PU with bioactive agents like chitosan or collagen (Maria et al. 2012). The mixture of biopolymers and synthetic ones can result in a synergistic effect of improved biocompatibility with easy processability and improved mechanical characteristics (Barikani et al. 2010). In this study, the contact angle of the PU and the developed patches revealed no significant disparity, even though slightly higher values were determined for the composite and even more after the coating with Hp. This might be caused by the hydrophobic character of the Cn (Liu et al. 2011; Mit-uppatham et al. 2004). In conclusion, a significant change could not be demonstrated in the wettability of the developed patch.

Scanning electron microscope

The surface characteristics of an electrospun patch used for ASD closure are essential with respect to the biocompatibility and cell adherence. The SEM allows an evaluation of the surface's topographical characteristics, e.g., roughness or presence of pits as well as the determination of the nanofiber diameter. Respective images are shown in Fig. 7. The diameter of the nanofiber of the PU reference was found to be 445.71 ± 34.89 nm, the PUCnCo fibers were slightly smaller with a mean diameter of 275 ± 61.65 nm, as displayed in Fig. 8. An even structure and uniform patch is another important factor which can have an impact on the biocompatibility of the patch, therefore the nanofiber diameter was evaluated. In accordance with a study of Kim et al. the PU nanofiber diameter ranged from 0.4 to 2.1 µm (Kim et al. 2009). Liu et al. developed a biodegradable occlusion device using electrospinning with PLGA and Co. They have shown that the diameter of the nanofibers ranged between 130 and 520 nm (Liu et al. 2011). The developed patches as well as the PU control patch are in the similar range reported in the above studies. The diameter of the composite nanofiber patch decreased compared to the PU reference. This can be due to the addition of Co which decreases the viscosity of the solution. The lower viscosity is caused by a reduction of the viscoelastic force and the Coulombic stretching. This fact leads to the observed reduction in the nanofiber diameter (Liu and Gao 2009; Li et al. 2008). The reduced diameter of the nanofibers leads into a smaller nanofiber matrix which may be linked to better cell proliferation and adhesion. Recently, Chen et al.

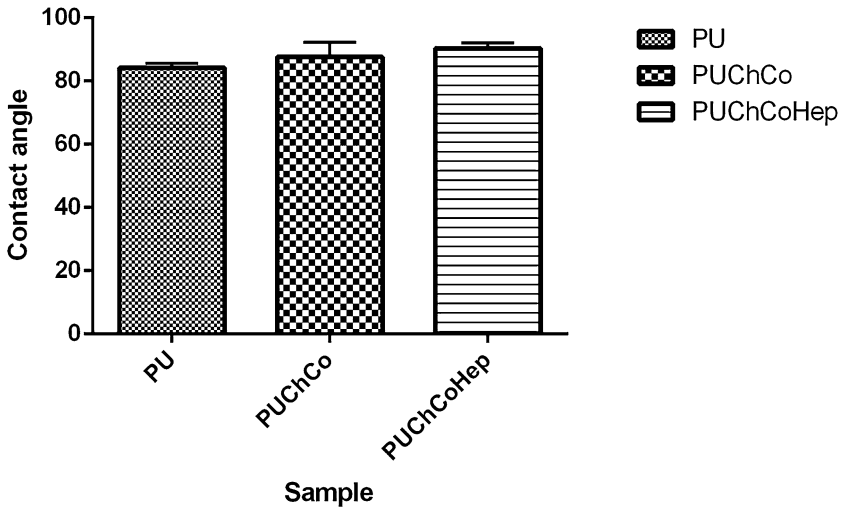

Fig. 6 Mean contact angle values of control, composite and coated samples with standard deviation

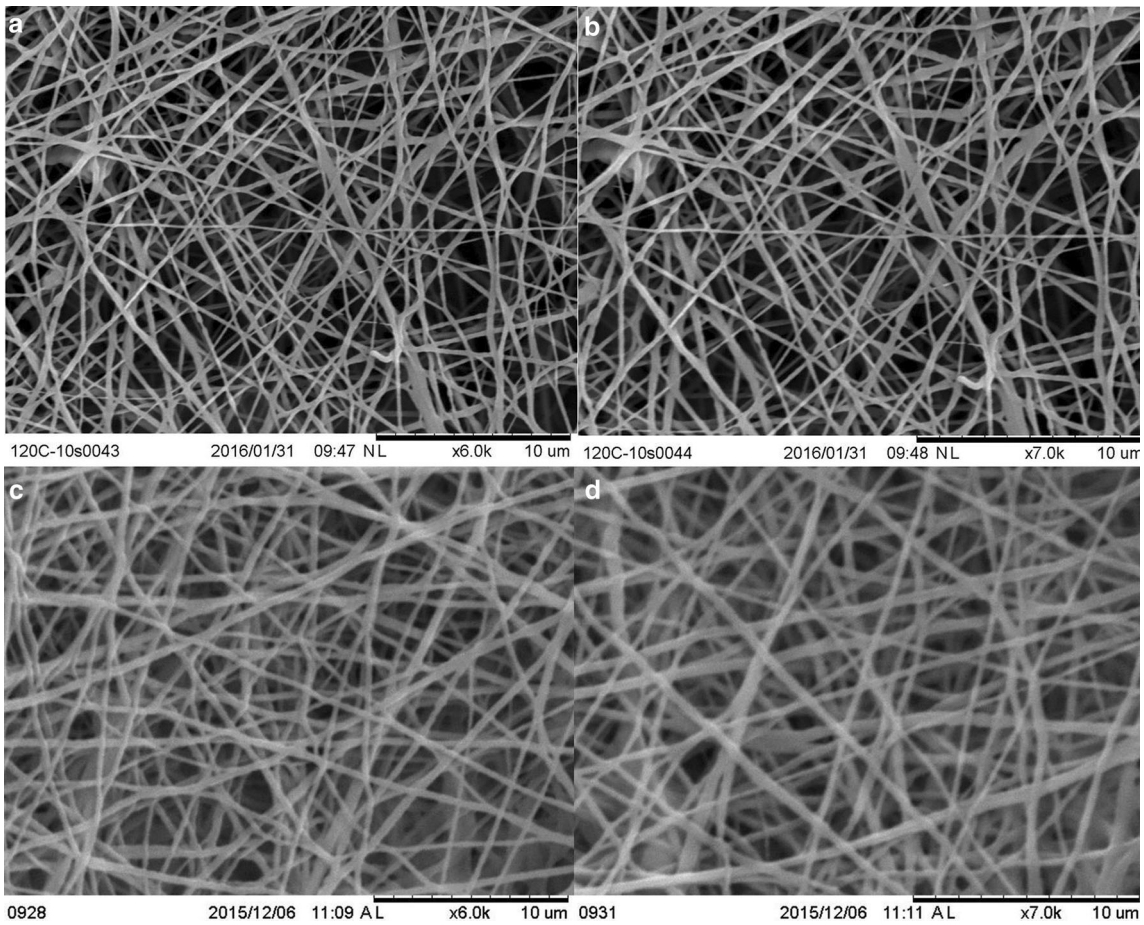

Fig. 7 **a**, **b** Electrospun PU patch SEM images at magnification of ×6000 and ×7000, respectively. **c**, **d** Electrospun PUChCo patch SEM images at magnification of ×6000 and ×7000, respectively

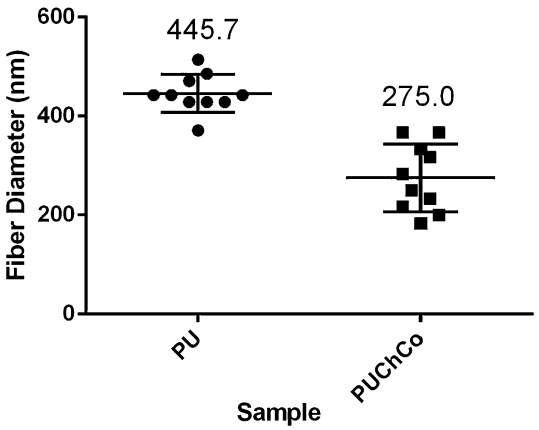

Fig. 8 Fiber diameters of the electrospun polymer sheets, displayed with their mean value as 445.7 for the PU patch and 275.0 for the composite. The standard deviation is shown, pointing out the uniformity of the patches

(2007) demonstrated the enhanced adhesion of fibroblasts on reduced nanofiber matrices. Similar findings were reported with neural stem cells (Christopherson et al. 2009). These observations which are in consensus with the result of this study bolster the feasibility of the fabricated electrospun nanofiber to be used for cardiac patch application. No bead formation was found for the PU control. In the PUCnCo slight bead formation could be determined, probably triggered by the diminution of the solution viscosity (Kim et al. 2009; Li et al. 2008). Regarding the structural uniformity, the distribution of the control fiber across the sheet is uniform, isotropic and homogeneous. The composite showed comparable good results as control.

Fluid uptake percentage

The fluid uptake was evaluated on the basis of three measuring points. The graphs depict that the pure PU patch shows a higher swelling ability than the composite patch. The mean fluid uptake of the PU was more than double the PUCnCo/PUCnCoHp uptake. The mean value for the fluid uptake for all three samples over the measurement points with standard deviation and significance is indicated in Fig. 9. The difference between the control and the samples fluid uptake indicates that the PU absorbs the fluid within a

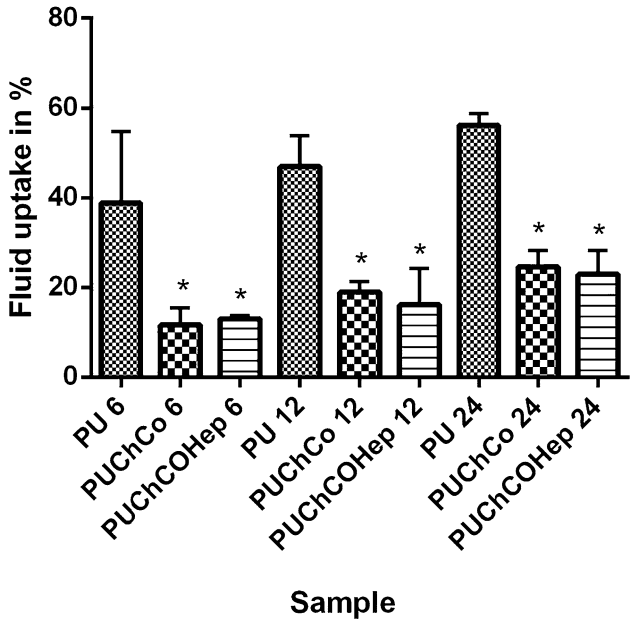

Fig. 9 Mean value for the fluid uptake for all three samples over the measurement points with standard deviation and significance indicated

significantly higher range ($p < 0.05$) than the composite for all three measuring points. For the two composites no significant difference could be found. Over the time span of 24 h, the fluid uptake was increased linearly. The linear gradient for PU is 0.94, for the PUCnCo is 0.69 and for the Hp-coated sample is 0.55. The fluid uptake test indicated that the PU can absorb fluid significantly compared to the composites ($p < 0.05$). The fluid uptake rate is an indicator for the biocompatibility of a patch. In this case, the FUA % significance might be caused by the hydrophobic character of the Cn. Regarding the difference between the uncoated and the coated patch, no significance is displayed. Even though the fluid uptake is an index for the biocompatibility in this application, a lower FUA % is sensible. Since, it is directly implanted in the blood circuit a high uptake might cause changes in the mechanical properties of the patch and might lead into its destruction.

Blood compatibility assessment

Activated partial thromboplastin time

Activated partial thromboplastin time assay was performed for the two composite patches and the control PU. The mean values are illustrated in Fig. 10a. The control PU sample had a mean clotting time of 72.92 ± 15.84 s. The PUCnCoHp showed a significant ($p < 0.05$) delay of clot formation while the uncoated composite patch showed no significant change. It even demonstrated a lower mean value compared to the control of 70.77 ± 4.06 s. The coated sample exhibited an increased clot formation time of 103.33 ± 4.75 s. APTT is utilized for studying the propensity of blood to coagulate via intrinsic pathway and to determine the effect of biomaterials on delaying the blood clotting process. This test is the most frequently used method to monitor anticoagulant response in clinical settings (Fong et al. 1999; Elahi et al. 2014). Hence, the increase of the APTT for the Hp-coated sample indicates a delay of the activation of the intrinsic pathway.

Prothrombin time

The PT is measured to analyze the impact the developed patches in the clot formation through the extrinsic pathway. As for the APTT, the experiment was carried out three times for each sample ($n = 3$). The PT is illustrated in Fig. 10b. Similar to the APTT only the coated sample showed a significant difference ($p < 0.05$) in comparison with the control PU. It was found to be 35.57 ± 2.74 s, compared to the control with a mean of 25.73 ± 2.32 s. The uncoated PUCnCo presented a mean value of 29.4 ± 0.59 s.

In contrast to the APTT, the PT measures the integrity of the extrinsic pathway. In this study, the PT was significantly increased for the Hp-coated patch and only slightly elevated for the PUChCo patch without any significance. This result is in corroboration with the results obtained in a work done by Yang et al. (2011), where the Hp coating prolongs the PT due to its antithrombogenicity. The composite PuChCoHp showed the highest PT, which leads to the assumption of the best blood compatibility among the different patches fabricated in this study.

Hemolysis ratio

The mean absorbance for the control was determined as 0.159. For the two composite patches it was 0.105 for the PUChCo and 0.094 for the PUCnCoHp, shown in Fig. 10c. The HR was then calculated with formula (1). For the control the mean was found as 3.64%, for the PUCnCo was 2.39% and PUCnCoHp was 2.12%. The hemolysis ratio indicates the compatibility of a biomaterial with RBC. When RBCs gets in contact with artificial material like the PU patch, the RBC membrane is exposed to a massive dynamic stress. To evaluate this osmotic stress on the RBCs, the hemolysis assay is performed (Vellayappan et al. 2016). According to the ASTM F 756-00 (2000) standard materials are classified into three categories according to their hemolytic ratio. If the percentage is above 5% materials are classified as hemolytic, if between 5 and 2% they are considered as moderately hemolytic and below 2% it is classified as non-hemolytic material. In this study, the hemolysis ratio was found to be 3.00, 2.61 and

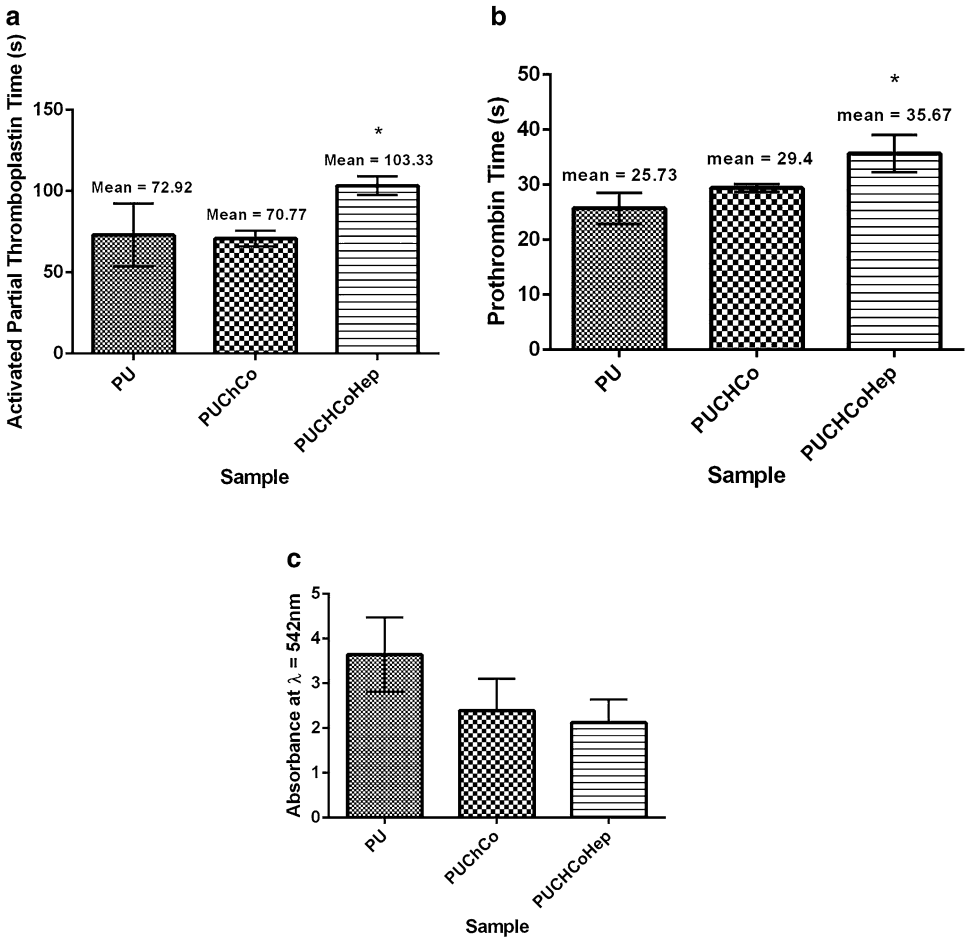

Fig. 10 **a**, **b** Mean value of APTT and PT in seconds with the standard deviation, significance highlighted with *asterisks* ($p < 0.05$). **c** Hemolysis ratio with standard deviation

2.33%, respectively, for the pristine PU, PUChCo and PUChCoHp patches. Since the ratio is beneath the mentioned mark of 5%, all the patches can be considered as compatible with RBCs. However, the PUChCoHp patches demonstrate the best result compared to other samples. Hence, the overall result of this study suggests that the novel PUChCoHp patches can be considered as a potential candidate for cardiac patch application.

Conclusion

A biodegradable patch for the occlusion of ASD was developed and tested. Developed composite patch displayed reduced fiber diameter compared to the pristine PU. FTIR analysis indicated the presence of functional groups unique to chitosan, collagen and heparin added in the composite. Contact angle and fluid uptake were in agreement to the desired properties of ASD patch. Further, coating of heparin on the composite patch delayed the APTT and PT significantly. Also, the hemolysis ratio was reduced expressing the feasibility of the developed patch for ASD occluder. Even though the results are promising, further in vivo tests need to be conducted to assure the abilities of the developed ASD patch before promoting it to clinical trials.

Acknowledgements This work was supported partly by the Ministry of Higher Education Malaysia with the Grant Vot number: Q.J130000.2545.12H80.

Compliance with ethical standards

Conflict of interest The authors declared no potential conflicts of interest with respect to the research, authorship, and/or publication of this article.

References

Amarnath LP, Srinivas A, Ramamurthi A (2006) In vitro hemocompatibility testing of UV-modified hyaluronan hydrogels. Biomaterials 27:1416–1424

Balaji A, Vellayappan MV, John AA et al (2015) An insight on electrospun nanofibers inspired modern drug delivery system in the treatment of dreadful cancers. RSC Adv 5:57984–58004

Barikani M, Honarkar H, Barikani M (2010) Synthesis and characterization of chitosan-based polyurethane elastomer dispersions. Monatshefte für Chemie Chem Mon 141:653–659

Chen M, Patra PK, Warner SB, Bhowmick S (2007) Role of fiber diameter in adhesion and proliferation of NIH 3T3 fibroblast on electrospun polycaprolactone scaffolds. J Tissue Eng 13:579–587

Chen J, Chen C, Chen Z, Chen J, Li Q, Huang N (2010) Collagen/heparin coating on titanium surface improves the biocompatibility of titanium applied as a blood-contacting biomaterial. J Biomed Mater Res A 95:341–349

Chen J, Huang N, Li Q, Chu CH, Li J, Maitz MF (2016) The effect of electrostatic heparin/collagen layer-by-layer coating degradation on the biocompatibility. Appl Surf Sci 362:281–289

Christopherson GT, Song H, Mao HQ (2009) The influence of fiber diameter of electrospun substrates on neural stem cell differentiation and proliferation. Biomaterials 30:556–564

Crawford GB, Brindis RG, Krucoff MW, Mansalis BP, Carroll JD (2012) Percutaneous atrial septal occluder devices and cardiac erosion: a review of the literature. Catheter Cardiovasc Interv 80:157–167

Detta N, Errico C, Dinucci D (2010) Novel electrospun polyurethane/gelatin composite meshes for vascular grafts. J Mater Sci Mater Med 21:1761–1769

Elahi MF, Guan G, Wang L (2014) Hemocompatibility of surface modified silk fibroin materials: a review. Adv Mater Sci 38:148–159

Eyre L, Gamlin F (2010) Haemostasis blood platelets and coagulation. Anaesth Intensive Care Med 11:244–246

Farzaneh S, Fitoussi J, Lucas A, Bocquet MT, Charkhtchi A (2013) Shape memory effect and properties memory effect of polyurethane. Appl Polym Sci 128:3240–3249

Fong H, Chun I, Reneker DH (1999) Beaded nanofibers formed during electrospinning. Polymer 40:4585–4592

Fornell D (2013) FDA reports serious erosion events with amplatzer septal occluder. https://www.dicardiology.com/article/fda-reports-serious-erosion-events-amplatzer-septal-occluder. Accessed Jan 2017

Gorbet MB, Sefton MV (2004) Biomaterial-associated thrombosis: roles of coagulation factors, complement, platelets and leukocytes. Biomaterials 25:5681–5703

Jaganathan SK, Mani MP, Ismail AF, Ayyar M (2017) Manufacturing and characterization of novel electrospun composite comprising polyurethane and mustard oil scaffold with enhanced blood compatibility. Polymers 9:163–173

Kim SE, Heo DN, Lee JB (2009) Electrospun gelatin/polyurethane blended nanofibers for wound healing. J Biomed Mater 4:044106

Klement P, Du YJ, Berry L, Andrew M, Chan AK (2002) Blood-compatible biomaterials by surface coating with a novel antithrombin–heparin covalent complex. Biomaterials 23:527–535

Korabathina R, Thaler DE, Kimmelstiel C (2012) Stroke due to late device thrombosis following successful percutaneous patent foramen ovale closure. Catheter Cardiovasc Interv 80:498–502

Li P, Dai YN, Zhang JP, Wang AQ, Wei Q (2008) Chitosan–alginate nanoparticles as a novel drug delivery system for nifedipine. Int J Biomed Sci 4:221–228

Liu H, Gao C (2009) Preparation and properties of ionically cross-linked chitosan nanoparticles. Polym Adv Tech 20:613–619

Liu SJ, Peng KM, Hsiao CY, Liu KS, Chung HT, Chen JK (2011) Novel biodegradable polycaprolactone occlusion device combining nanofibrous PLGA/collagen membrane for closure of atrial septal defect (ASD). Ann Biomed Eng 39:2759–2766

Lorevice MV, Otoni CG, Moura MRD, Mattoso LHC (2015) Chitosan nanoparticles improving mechanical properties of different pectin-based films: low and high methoxyl degrees. J Mater Sci Eng 4:124

Manikandan A, Mani MP, Jaganathan SK, Rajasekar R, Jagannath M (2017) Formation of functional nanofibrous electrospun polyurethane and murivenna oil with improved haemocompatibility for wound healing. Polym Test 61:106–113

Maria OB, Doina M, Cristina D, Laura K, Valeria H (2012) Biocompatibility and biological performance of the improved polyurethane membranes for medical applications. Intech Publishers, Rijeka

Mit-uppatham C, Nithitanakul M, Supaphol P (2004) Ultrafine electrospun polyamide-6 fibers: effect of solution conditions on morphology and average fiber diameter. Macromol Chem Phys 205:2327–2338

Moura MR, Avena-Bustillos RJ, McHugh TH, Krochta JM, Mattoso LH (2008) Properties of novel hydroxypropyl methylcellulose films containing chitosan nanoparticles. J Food Sci 73:31–37

Moura MR, Aouada FA, Avena-Bustillos RJ, McHugh TH, Krochta JM, Mattoso LH (2009) Improved barrier and mechanical properties of novel hydroxypropyl methylcellulose edible films with chitosan/tripolyphosphate nanoparticles. J Food Eng 92:448–453

Pedicini A, Farris RJ (2003) Mechanical behavior of electrospun polyurethane. Polymer 44:6857–6862

Qi L, Xu Z, Jiang X, Hu C, Zou X (2004) Preparation and antibacterial activity of chitosan nanoparticles. Carbohydr Res 339:2693–2700

Rinaudo M (2006) Chitin and chitosan: properties and applications. Prog Polym Sci 31:603–632

Sill TJ, Recum HA (2008) Electrospinning: applications in drug delivery and tissue engineering. Biomaterials 29:1989–2006

Thirumal M, Khastgir D, Singha NK, Manjunath BS, Naik YP (2008) Effect of foam density on the properties of water blown rigid polyurethane foam. J Appl Polym Sci 108:1810–1817

Vellayappan MV, Jaganathan SK, Muhammad II (2016) Unravelling the potential of nitric acid as a surface modifier for improving the hemocompatibility of metallocene polyethylene for blood contacting devices. PeerJ 4:e1388

Wang A, Xu C, Zhang C, Gan Y, Wang B (2015) Experimental investigation of the properties of electrospun nanofibers for potential medical application. J Nanomater 2015:8

Wertman B, Azarbal B, Riedl M, Tobis J (2006) Adverse events associated with nickel allergy in patients undergoing percutaneous atrial septal defect or patent foramen ovale closure. J Am Coll Cardiol 47:1226–1227

Wong CS, Badri KH (2012) Chemical analyses of palm kernel oil-based polyurethane prepolymer. Mater Sci Appl 3:78–86

Wright JI (2006) Using polyurethanes in medical applications. http://www.mddionline.com/article/using-polyurethanes-medical-applications. Accessed Jan 2017

Yang H, Xu H, Liu H, Ouyang C, Xu W (2011) A novel heparin release system based on blends of biomedical polyurethane and native silk fibroin powder. J Control Release 152:106–108

Zhou FL, Gong RH (2008) Manufacturing technologies of polymeric nanofibres and nanofibre yarns. Polym Int 57:837–845